http://dx.doi.org/10.5012/bkcs.2013.34.9.2609

Synthesis and Characterization of Red Electrophosphorescent Polymers Containing Pendant Iridium(III) Complex Moieties

Fei Xu, Dongbo Mi, Hong Ryeol Bae,† Min Chul Suh,† Ung Chan Yoon, and Do-Hoon Hwang*

Department of Chemistry, and Chemistry Institute for Functional Materials, Pusan National University, Busan 609-735, Korea
**E-mail: dohoonhwang@pusan.ac.kr*
†Department of Information Display and Advanced Display Research Center, Kyung Hee University, Seoul 130-701, Korea
Received April 16, 2013, Accepted June 6, 2013

A series of fluorene-carbazole copolymers containing the pendant phosphor chromophore $Ir(absn)_2(acac)$ (absn: 2-(1-naphthyl)benzothiazole; acac: acetylacetone) were designed and synthesized *via* Yamamoto coupling. In the film state, these copolymers exhibited absorption and emission peaks at approximately 389 and 426 nm, respectively, which originated from the fluorene backbone. However, in electroluminescent (EL) devices, a significantly red-shifted emission at approximately 611 nm was observed, which was attributed to the pendant iridium(III) complex. Using these copolymers as a single emission layer, polymer light-emitting devices with ITO/PEDOT:PSS/polymer:DNTPD/TmPyPb/LiF/Al configurations exhibited a saturated red emission at 611 nm. The attached iridium(III) complex had a significant effect on the EL performance. A maximum luminous efficiency of 0.85 cd/A, maximum external quantum efficiency of 0.77, maximum power efficiency of 0.48 lm/W, and maximum luminance of 883 cd/m^2 were achieved from a device fabricated with the copolymer containing the iridium(III) complex in a 2% molar ratio.

Key Words : Fluorene, Iridium(III) complex, Phosphorescent polymer light-emitting device

Introduction

Polymer light-emitting diodes (PLEDs) based on phosphorescent heavy-metal complexes have recently attracted significant attention for next-generation displays and solid-state lighting technologies, because 100% internal quantum efficiency can theoretically be achieved and they can be fabricated through cost-effective solution processes such as spin-coating or ink-jet printing.[1,2] In general, two strategies are used to generate phosphorescent polymer light-emitting diodes (PhPLEDs). One method involves physically blending the phosphor with the polymer host. Although highly efficient PhPLEDs have been achieved using this method,[3] potential problems such as aggregation and phase separation could diminish the lifetime and stability of the emission color of the devices.[4-6] Therefore, a second method that involves chemically attaching the phosphor to the polymer host was recently developed to overcome these issues. In previous reports, phosphorescent metal complexes were incorporated into the polymer main chain, grafted into the side chain, or hyper-branched into the polymer chain.[7-9] Some green hyper-branched polymers with high efficiencies[10] and a few efficient red phosphorescent polymers have been reported thus far.

The most widely used polymer hosts are poly(2,7-fluorene)s (PFs) and their derivatives, owing to their wide band gaps, high photoluminescence (PL) quantum efficiencies, and excellent conductivities. However, PFs are not considered as suitable hosts for red phosphorescent polymers because the triplet energy states (E_T) of PFs occur at 2.15-2.3 eV,[11] and are similar to those of typical red phosphorescent iridium complexes. However, in 2006, Holmes and co-workers reported a series of polyfluorene copolymers with red-emitting iridium complexes attached either directly or through a spacer; they proposed that Dexter triplet-energy back transfer could be inhibited by increasing the distance between the host and the iridium complex.[12]

In this study, we designed and synthesized a series of fluorene-carbazole copolymers with red-emitting $Ir(absn)_2$-acac complex (absn: 2-(1-naphthyl)benzothiazole; acac: acetylacetone) grafted into the side chain. $Ir(absn)_2acac$, which has an efficient, broad red emission,[13] was introduced through a $-(CH_2)_8-$ chain at the 9-position of the carbazole host. The guest and host monomers were copolymerized in varying monomer ratios using the Yamamoto polycondensation. The synthetic routes and chemical structures of the polymers are shown in Scheme 1. The thermal, electrochemical, photophysical, and electroluminescence properties of the copolymers will be discussed.

Experimental

Materials. Iridium(III) chloride, carbazole, and fluorene were purchased from Alfa Aesar, and acetylacetone was purchased from ACROS. 1-Naphthaldehyde and 2-aminothiophenol were obtained from Aldrich. Bis(1,5-cyclooctadiene)nickel(0) [$Ni(COD)_2$] was purchased from Strem. All reagents were used without further purification. 2-Ethoxyethanol was obtained from Junsei, anhydrous toluene was purchased from Aldrich, and *N,N*-dimethylformamide (DMF) was obtained from Alfa Aesar. 2-Ethoxyethanol was used after purging with dry nitrogen for 1 h. 2-(1-Naphthyl)-

benzothiazole,[13] 2,7-dibromo-9,9-bis(4-octyloxyphenyl)-fluorene,[8] and 3,6-dibromo-9-(tridecane-10,12-dionyl)-9*H*-carbazole[14] were prepared according to literature procedures. All manipulations involving $IrCl_3 \cdot 3H_2O$ and other Ir(III) species were performed in a dry nitrogen atmosphere.

Synthesis of 3,6-Dibromo-9-((iridium(III)bis(2-(1-naphthyl)benzothiazine-*N*,$C^{2'}$))-tridecane-10,12-dionyl)carbazole (1). The cyclometalated Ir(III) μ-chloro dimer was synthesized *via* the method reported by Nonoyama.[15] Iridium(III) chloride (0.75 g, 2.5 mmol) and 2-(1-naphthyl)benzothiazole (1.5 g, 5.7 mmol) were added to a mixture of 2-ethoxyethanol and water (30 mL, 3:1, v/v) and refluxed at 125 °C for 12 h under a N_2 atmosphere. The solution was cooled to room temperature, and the resultant precipitate was collected and washed several times with water and petroleum ether to afford a dark-brown powder. The solid was dried *in vacuo* to give the cyclometalated iridium(III) μ-chloro dimer in a 74.3% yield. 3,6-Dibromo-9-(tridecane-10,12-dionyl)-9*H*-carbazole (0.59 g, 1.1 mmol), sodium carbonate (0.25 g, 2.3 mmol), and cyclometalated iridium(III) μ-chloro dimer (0.7 g, 0.5 mmol) were dissolved in 2-ethoxyethanol and refluxed for 12 h under a nitrogen atmosphere. After the crude solution was cooled to room temperature, it was poured into water, extracted with dichloromethane, dried over anhydrous magnesium sulfate, and concentrated *in vacuo*. The residue was purified *via* silica gel column chromatography with a dichloromethane and hexane (1:1) mixture as the eluent, and then recrystallized from a mixture of dichloromethane and hexane; a dark red solid complex was obtained in 36% yield. ^{1}H NMR (300 MHz, $CDCl_3$) δ 8.60 (d, 1H), 8.52 (d, 1H), 8.16 (s, 2H), 8.08 (d, 2H), 8.00 (d, 1H), 7.88 (d, 1H), 7.66-7.51 (m, 6H), 7.46-7.29 (m, 6H), 7.27 (d, 2H), 7.00 (t, 2H), 6.65 (d, 1H), 6.56 (d, 1H), 5.05 (s, 1H), 4.22 (t, 2H), 1.89 (m, 2H), 1.79 (t, 2H), 1.74 (s, 3H), 1.26-0.95 (m, 10H).

Synthesis of the Polyfluorene Derivative with 1 mol % Feed Ratio of the Iridium Complex (PFIrabsn1). 2,7-Dibromo-9,9-bis(4-octyloxyphenyl)fluorene (0.8 g, 1.09 mmol), 3,6-dibromo-9-((iridium(III)bis(2-(1-naphthyl)benzothiazine-*N*,$C^{2'}$))-tridecane-10,12-dionyl)carbazole (13.8 mg, 0.01 mmol), $Ni(COD)_2$ (0.46 g, 1.67 mmol), and 2,2'-dipyridyl (0.28 g, 1.79 mmol) were dissolved in a mixture of toluene and DMF (10 mL, 1:1, v/v) and stirred for 0.5 h. 1,5-Cyclooctadiene (0.20 mL) was added to the reaction mixture under an argon atmosphere. The resulting solution was stirred at 80 °C for 36 h, and then excess bromobenzene dissolved in anhydrous toluene (1 mL) was added to cap the end groups. The reaction mixture was stirred for an additional 12 h, then cooled to room temperature and slowly poured into methanol (200 mL). The polymer was collected by filtration and purified by silica gel column chromatography using chloroform as the eluent to remove the low-molecular-weight oligomers and catalyst residues. The polymer was then further purified by Soxhlet extraction with acetone as the solvent. The resulting polymer was soluble in common organic solvents, including chloroform and toluene. The polymer yield was 52%. ^{1}H NMR (300 MHz, $CDCl_3$) δ 8.33 (br, 0.01H), 7.76 (d, 2H), 7.55 (br, 4H), 7.17 (d, 4H), 6.77 (d, 4H), 5.05 (br, 0.01H), 3.88 (br, 4H), 1.73 (br, 4H), 1.41-1.27 (br, 20H), 0.87 (br, 6H).

Synthesis of PFIrabsn0. 2,7-Dibromo-9,9-bis(4-octyloxyphenyl)fluorene (0.8 g, 1.09 mmol) was used for the polymerization. Yield: 28%. ^{1}H NMR (300 MHz, $CDCl_3$) δ 7.76 (d, 2H), 7.55 (br, 4H), 7.17 (d, 4H), 6.77 (d, 4H), 3.88 (br, 4H), 1.73 (br, 4H), 1.41-1.26 (br, 20H), 0.87 (br, 6H).

Synthesis of PFIrabsn2. 2,7-Dibromo-9,9-bis(4-octyloxyphenyl)fluorene (0.8 g, 1.09 mmol) and 3,6-dibromo-9-((iridium(III)bis(2-(1-naphthyl)-benzothiazine-*N*,$C^{2'}$))-tridecane-10,12-dionyl)carbazole (27.8 mg, 0.02 mmol) were used for the polymerization. Yield: 53%. ^{1}H NMR (300 MHz, $CDCl_3$) δ 8.33 (br, 0.03H), 7.76 (d, 2H), 7.55 (br, 4H), 7.17 (d, 4H), 6.77 (d, 4H), 5.05 (br, 0.02H), 3.90 (br, 4H), 1.73 (br, 4H), 1.41-1.26 (br, 20H), 0.87 (br, 6H).

Synthesis of PFIrabsn5. 2,7-Dibromo-9,9-bis(4-octyloxyphenyl)fluorene (0.75 g, 1.02 mmol) and 3,6-dibromo-9-((iridium(III)bis(2-(1-naphthyl)-benzothiazine-*N*,$C^{2'}$))-tridecane-10,12-dionyl)carbazole (67.2 mg, 0.05 mmol) were used for the polymerization. Yield: 28%. ^{1}H NMR (300 MHz, $CDCl_3$) δ 8.34 (br, 0.06H), 7.76 (d, 2H), 7.55 (br, 4H), 7.17 (d, 4H), 6.77 (d, 4H), 5.05 (br, 0.03H), 3.89 (br, 4H), 1.73 (br, 4H), 1.41-1.26 (br, 20H), 0.87 (br, 6H).

Device Fabrication. Devices with ITO/PEDOT:PSS/polymer:DNTPD/TmPyPb/LiF/Al configurations were fabricated using each of the synthesized polymers, as follows: Indium tin oxide (ITO) glass substrates were consecutively washed with acetone, detergent, distilled water, and 2-propanol. After treatment with oxygen plasma for 25 min, a 60 nm thick layer of poly(3,4-ethylenedioxythiophene) doped with poly(styrenesulfonic acid) (PEDOT:PSS, Bayer AG, Germany) was spin-coated onto the ITO substrates. The spin-coated film was baked in air at 120 °C for 20 min. The light-emitting polymer and *N,N'*-bis-[4-(di-*m*-tolylamino)-phenyl]-*N,N'*-diphenylbiphenyl-4,4-diamine (DNTPD) (in a 1:1 weight ratio) were then dissolved in chlorobenzene, filtered through a 0.50 μm PTFE (hydrophobic) syringe filter, and spin-coated onto the PEDOT:PSS layer. The active layer was around 30 nm thick, as determined using an Alpha-Step IQ surface profiler (KLA Tencor). After spin-coating, the devices were immediately transferred into a vacuum chamber where they were annealed at 80 °C for 30 min to remove residual chlorobenzene. Then, a 30 nm thick 1,3,5-tri[(3-pyridyl)-phen-3-yl]benzene (TmPyPb) electron transport layer, a 1 nm thick LiF layer, and a 100 nm thick Al layer were thermally deposited at a pressure of $\sim 1 \times 10^{-7}$ Torr.

Measurements. ^{1}H NMR spectra were recorded in $CDCl_3$ on a Varian Mercury 300 MHz spectrometer. The number- and weight-average molecular weights (M_n and M_w, respectively) and the polydispersity indices (PDIs) of the polymers were determined *via* gel permeation chromatography (GPC) analysis relative to a polystyrene standard using a Waters high-pressure GPC assembly (model M590). Thermogravimetric analysis (TGA) was performed on a LABSYS analyzer (SETARAM instrumentation) under nitrogen atmosphere at a heating rate of 10 °C min^{-1}. Ultraviolet (UV)-visible

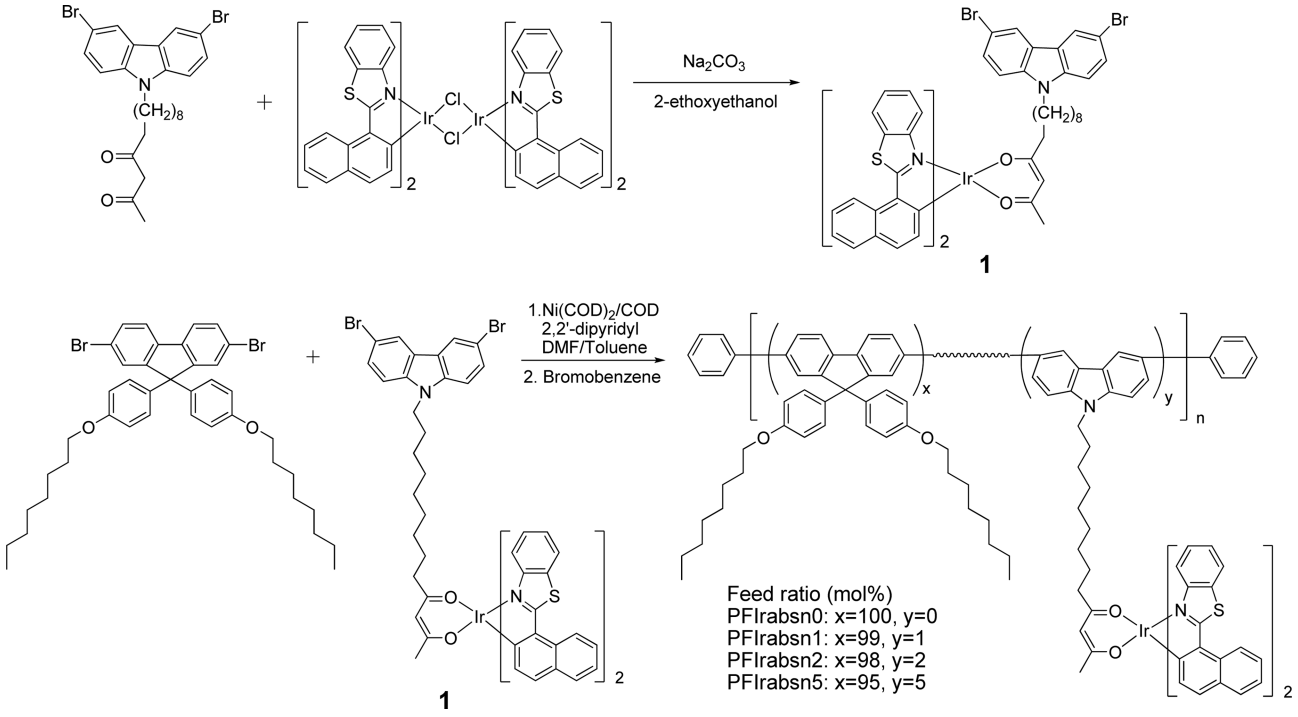

Scheme 1. Synthetic routes to iridium complex and copolymers.

absorption was recorded using a Scinco S-3100 UV-visible spectrophotometer. Photoluminescence emission spectra were recorded using a Hitachi F-7000 fluorescence spectrophotometer. The excitation wavelengths for the monomer and the copolymers were 400 nm and 350 nm, respectively. Cyclic voltammetry (CV) was carried out in acetonitrile (CH_3CN) solution containing 0.1 M tetrabutylammonium tetrafluoroborate ($TBABF_4$) as the supporting electrolyte using a CH Instruments electrochemical analyzer with a $Ag/AgNO_3$ reference electrode and a platinum wire counter electrode. Electroluminescence (EL) spectra and CIE coordinates were obtained using a Minolta CS-1000 spectroradiometer. Current–voltage–luminance (*I–V–L*) characteristics were recorded using Keithley 2635A and Minolta CS-100A instruments.

Results and Discussion

Synthesis and Characterization. The synthetic routes for the iridium complex monomer and corresponding electrophosphorescent polymers are depicted in Scheme 1. 2-(1-Naphthyl)benzothiazole,[13] 2,7-dibromo-9,9-bis(4-octyloxyphenyl)fluorene,[8] and 3,6-dibromo-9-(tridecane-10,12-dionyl)-9*H*-carbazole[14] were synthesized according to reported procedures. The structure of the obtained iridium complex monomer **1** was confirmed by ^{1}H NMR as shown in Figure 1. The characteristic protons H_a and $H_{a'}$ from the absn ligand, H_n from the acac ancillary ligand, and H_o from the alkyl chain of the carbazole group were clearly observed at 8.60, 8.52, 5.05, and 4.21 ppm, respectively. The integral ratios of the protons were in good accordance with the monomer structure.

The copolymers were prepared *via* Yamamoto polymerization and end-capped with excess bromobenzene. The feed ratios of 3,6-dibromo-9-((iridium(III)bis(2-(1-naphthyl)benzothiazine-*N*,C$^{2'}$))-tridecane-10,12-dionyl)carbazole to 2,7-dibromo-9,9-bis(4-octyloxyphenyl)fluorene were 0, 1, 2, and 5 mol %; the corresponding polymers were designated as PFIrabsn0, PFIrabsn1, PFIrabsn2, and PFIrabsn5. The actual compositions of the synthesized copolymers were determined using ^{1}H NMR spectroscopy. The ratio of the ^{1}H NMR signal at 5.05 ppm, which was assigned to the proton on the acac ligand of the iridium monomer **1**, to the signal at 3.88 ppm, which was assigned to the protons of the alkyl chains of fluorene, was used to estimate the actual content of iridium complex in the copolymers. The feed ratios and

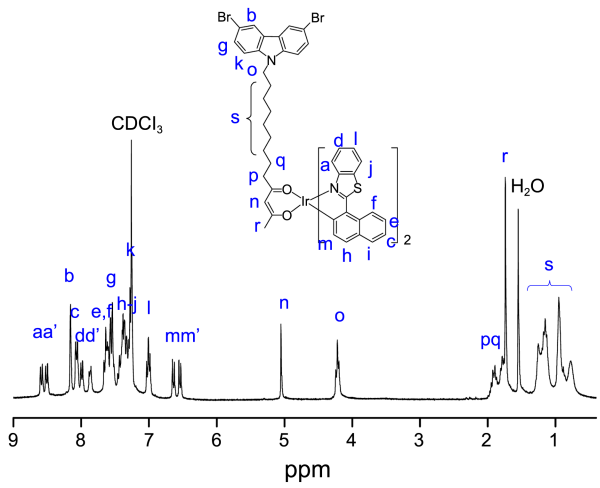

Figure 1. ^{1}H NMR spectrum of monomer **1**.

Table 1. Structural and thermal properties of copolymers

Copolymer	M_n[a] (×10³)	M_w[a] (×10³)	PDI	Host/Ir complex (mol %)[b]		T_d[c] (°C)
				feed ratio (%)	actual ratio (%)	
PFIrabsn0	10.2	26.2	2.56	100/0	100/0	430
PFIrabsn1	28.5	75.4	2.64	99/1	99.5/0.5	417
PFIrabsn2	23.2	54.8	2.36	98/2	98.5/1.5	408
PFIrabsn5	14.7	37.1	2.52	95/5	97.1/2.9	402

[a]Molecular weights were determined by GPC using polystyrene standards. [b]The iridium contents in copolymers were estimated by ^{1}H NMR. [c]Obtained from TGA measurements. T_d values were recorded at 5% weight loss.

actual contents of the iridium complex are listed in Table 1. Similar to other reported iridium-containing polymers,[16] the actual contents of the iridium complex in the copolymers were lower than the monomer feed ratios; this was possibly because of the low reactivity of the iridium complex monomer toward Yamamoto coupling. As determined by GPC, the M_n values were 10,200-28,500 with PDIs of 2.4-2.6 for the copolymers (Table 1). The thermal properties of the synthesized polymers, assessed by TGA in a nitrogen atmosphere, are shown in Table 1. The decomposition temperatures of the copolymers were relatively high (T_d: 430-400 °C). The detailed structural and thermal properties of the copolymers are summarized in Table 1.

Optical and Electrochemical Properties. Figure 2 shows the UV–visible absorption and PL emission spectra of the iridium complex monomer 1 in dichloromethane solution at room temperature. The strong absorptions at 273 and 303 nm correspond to the $^1\pi$-π^* transition from the carbazole unit and the cyclometalated ligand absn.[17] The absorptions at 320-400 and 450-550 nm correspond to the spin-allowed metal-to-ligand (^{1}MLCT) transition and the spin-forbidden metal-to-ligand (^{3}MLCT) transition, respectively.[13] The maximum PL emission and a shoulder PL emission of monomer **1** were observed at 611 and 663 nm, respectively, at room temperature. The measured E_T of monomer **1** was 2.03 eV.

The UV-visible absorption spectra of the copolymer thin films are shown in Figure 3(a). The characteristic absorption

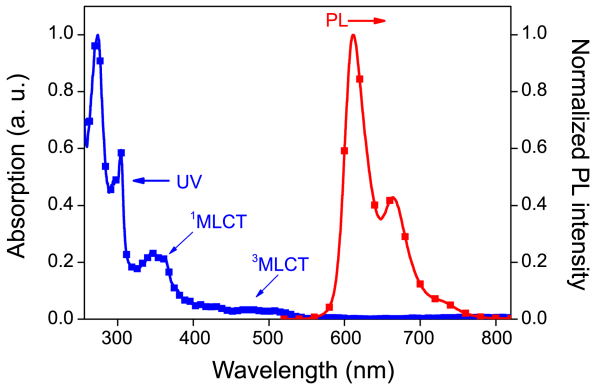

Figure 2. UV-visible absorption and PL spectra of monomer **1**.

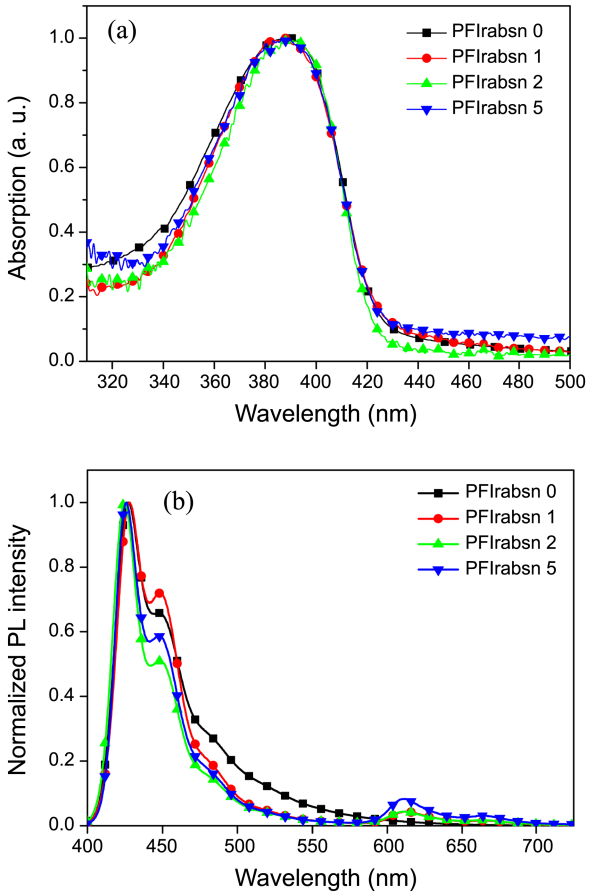

Figure 3. (a) UV-visible absorption and (b) PL spectra of copolymer films.

bands corresponding to the π-π^* transitions of the conjugated backbones were observed at 320-440 nm. The absorption of the iridium complex was buried in the absorption bands of the polymer main chains because of its low content. As the ratios of iridium complex in the copolymer increased, the position of the onset absorption did not appear to move to a longer wavelength.

Figure 3(b) shows the PL spectra of the copolymer thin films. The copolymer emissions were dominant at 426 nm with a small shoulder at 612 nm. The emission peaks at 426 nm were attributed to the fluorene host, and the 612 nm peaks were ascribed to the grafted absn complex. The relative intensities of the peaks at 426 nm remained almost independent of the Ir-complex content of the copolymers, but the red emission at 612 nm gradually increased as the Ir complex content increased. However, compared with the blue emissions from the host units, the red emissions from the Ir complexes were quite weak in the film state.

The electrochemical properties of the copolymers were studied by CV and are listed in Table 2. The copolymers showed oxidation waves with onsets between 1.09-1.12 V of the oxidation potential for the PFIrabsn copolymers, depending on the copolymer compositions. According to the literature, the HOMO level can be estimated from the onset oxidation potentials using the following equation: HOMO =

Table 2. Optical, electrochemical, and EL performances of devices containing copolymers

Copolymer	λ_{max}abs[a] [nm]	λ_{PL}[a] [nm]	HOMO[b] [eV]	LUMO[c] [eV]	$V_{turn\text{-}on}$[d] [V]	λ_{max} EL [nm]	CIE[e] [x, y]	L_{max} [cd/m^2]	EQE_{max} [%]	LE_{max} [cd/A]	PE_{max} [lm/w]
PFIrabsn0	389	427(448)	-5.83	-2.93	5.0	516	(0.27, 0.38)	205	0.13	0.22	0.08
PFIrabsn1	389	428(448), 612	-5.81	-2.91	3.5	507	(0.26, 0.38)	661	0.33	0.55	0.33
PFIrabsn2	389	425(447), 612	-5.83	-2.92	3.5	611	(0.57, 0.36)	883	0.77	0.85	0.48
PFIrabsn5	389	426(447), 611	-5.80	-2.89	3.5	611	(0.55, 0.33)	404	0.74	0.57	0.32

[a]Measured in film. [b]HOMO levels were calculated from CV potentials using ferrocene as a standard [HOMO= $-(4.8 + E_{ox,onset} - E_{Fc})$ eV]. [c]LUMO levels were derived *via* eq. E_g = HOMO-LUMO, where E_g obtained from the absorption spectra. [d]The voltage at a luminance of 1 cd/m^2. [e]At the maximum luminous efficiency.

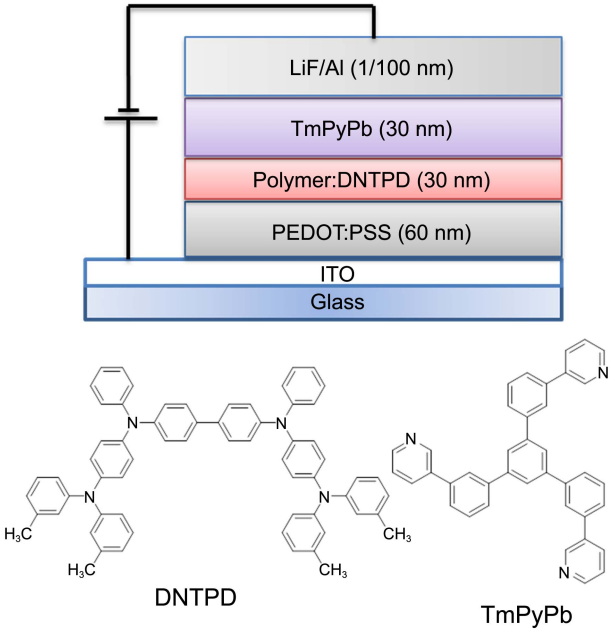

Figure 4. Schematic of device structure and chemical structures of materials used in PhPLEDs.

$(4.8 + E_{ox,onset} - E_{Fc})$, where $E_{ox,onset}$ and E_{Fc} are the onset oxidation potentials of the polymers and ferrocene, respectively.[18] The HOMO levels were calculated to be −5.80 to −5.83 eV, while the LUMO levels were −2.89 to −2.93 eV. The iridium complex content did not significantly affect the HOMO and LUMO levels of the copolymers.

Device Properties. Electroluminescent devices with ITO/PEDOT:PSS/polymer:DNTPD/TmPyPb/LiF/Al configurations were fabricated, as shown in Figure 4. To balance the carrier transport, a well-known electron transporting molecule, DNTPD,[19] was blended with the copolymers, which exhibited good hole-transporting properties, in a 1:1 weight ratio. TmPyPb was used as the electron-transporting layer.

The EL spectra of the fabricated devices are shown in Figure 5. The red emission band from the iridium complex was very weak in the PL spectra because of incomplete energy transfer from the main chain polymer host to the iridium complex in the side chain. In contrast to the PL spectra of the copolymers, the EL spectra shifted to longer wavelengths as the content of iridium complex in the copolymers increased. When the content of the iridium-containing monomer was higher than 1%, the emission at

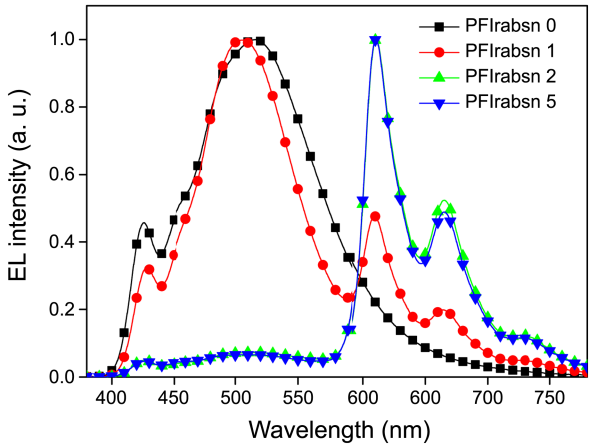

Figure 5. EL spectra of devices incorporating the copolymers.

around 611 nm clearly appeared. The emission of the fluorene host was almost quenched when the content of the grafted iridium complex reached 2 mol %. The substantial differences in the PL and EL spectra indicated that the predominant mechanism of the EL devices was charge trapping rather than energy transfer. The energy transfer process from the single excitons formed by photo-excitation of the host polymer to the triplet state of the iridium complex (by Förster energy transfer) would not be efficient in our host-guest system.[20] However, the excitons formed by electrical injection could be trapped in the iridium complex because of the difference in the HOMO/LUMO energy levels of the host and guest. Therefore, emission would

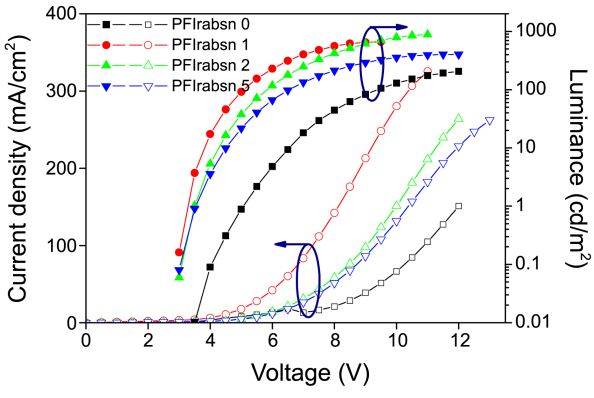

Figure 6. *I–V–L* curves of devices fabricated using copolymers.

occur predominantly at the red iridium complex in the EL devices. The EL spectra of devices using PFIrabsn2 and PFIrabsn5 copolymers as the emissive layers exhibited peak emissions at 611 nm, whereas a white emission with CIE coordinates of (0.26, 0.38) was observed from the device with copolymer PFIrabsn1. The latter result indicates that pure white emission can be achieved by tuning the content of the grafted iridium complex. Two simultaneous emissions from the host (*i.e.*, blue emission) and the grafted iridium complex (*i.e.*, broad red emission) can be expected.

The current density–voltage–luminance characteristics of the copolymers are shown in Figure 6. Low PhPLED turn-on voltages in the range of 3.5-5 V were observed, which can be attributed to the good charge injection of the device. The turn-on voltage of the PFIrabsn0 device was 5.0 V, while the turn-on voltages were 3.5 V for other devices regardless of the iridium contents in the copolymers. The current densities of the devices using the iridium-containing copolymers (PFIrabsn1, PFIrabsn2, and PFIrabsn5) were higher than that of the PFIrabsn0 device, as shown in Figure 6. The highest luminance, *i.e.*, 883 cd/m^2, was observed with the PFIrabsn2 copolymer.

The luminous efficiencies (LEs) and power efficiencies (PEs) as functions of luminance are shown in Figures 7(a) and 7(b). Among the four copolymers, the best device performance was observed with PFIrabsn2. A maximum quantum efficiency (EQE) of 0.77%, maximum LE of 0.85 cd/A, and maximum PE of 0.48 lm/W with a maximum brightness of 883 cd/m^2 were observed using this polymer, which had CIE coordinates of (0.57, 0.36). In particular, the luminous efficiencies of the EL device fabricated with PFIrabsn2 were almost constant with increasing luminance from 60 to 200 cd/m^2. This indicated that grafting the phosphorescent complexes into the polymer backbone *via* a long alkyl side chain could inhibit the efficiency roll-off, even at high current density,[21] because the Dexter energy transfer could be inhibited by increasing the distance between the host and iridium complex and the distance between the iridium complexes.[12] White light with CIE coordinates of (0.26, 0.38) was observed from the PhPLED fabricated with PFIrabsn1. The white PhPLEDs exhibited a maximum EQE of 0.33%, maximum LE of 0.55 cd/A, and maximum PE of 0.33 lm/W with a maximum brightness of 661 cd/m^2. The performances of the fabricated devices are summarized in Table 2.

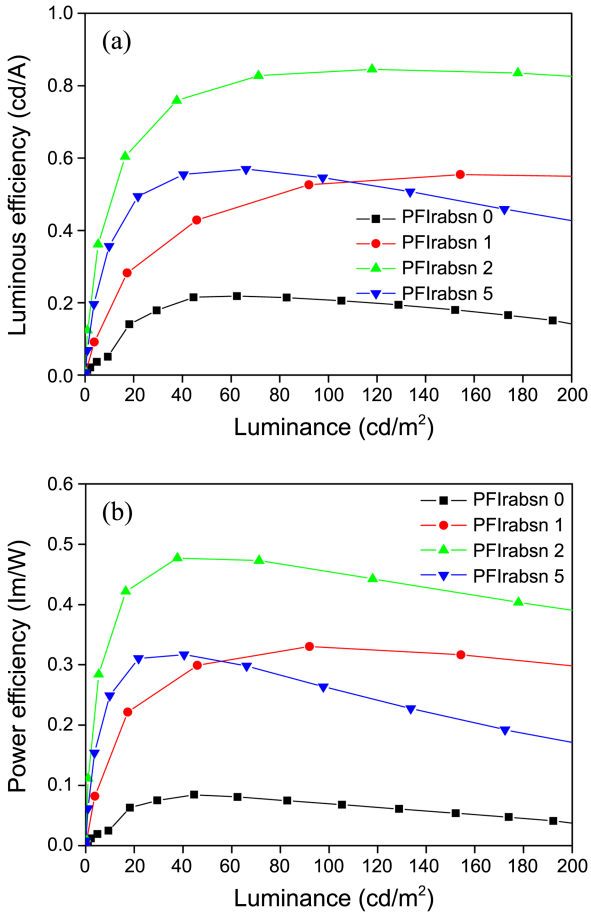

Figure 7. (a) Luminous efficiency–luminance and (b) power efficiency–luminance curves of copolymers.

Conclusion

A series of new phosphorescent polymers containing red-emitting iridium complexes were designed and synthesized. Each iridium complex was grafted through a long alkyl chain at the 9-position of carbazole, which was copolymerized with fluorene. By grafting the iridium complex through a tethering group, Dexter energy back-transfer was impaired and stable red emissions were observed. White emission was observed from the PFIrabsn1 copolymers, which demonstrated that high-performance white PhPLEDs could be obtained using a single copolymer with pendant iridium complexes.

Acknowledgments. This work was supported by a National Science Foundation (NRF) grant funded by the Korean government (MEST) (No. 2011-0011122) and the Industrial Strategic Technology Development Program (No. 10039141, Development of core technologies for organic materials applicable to OLED lighting with high color rendering index) funded by the Ministry of Knowledge Economy (MKE, Korea).

References

1. Baldo, M. A.; O'Brien, D. F.; You, Y.; Shoustikov, A.; Sibley, S.; Thompson, M. E.; Forrest, S. R. *Nature* **1998**, *395*, 151.
2. O'Brien, D. F.; Baldo, M. A.; Thompson, M. E.; Forrest, S. R. *Appl. Phys. Lett.* **1999**, *74*, 442.
3. Yang, C. L.; Zhang, X. W.; You, H.; Zhu, L. Y.; Chen, L. Q.; Zhu, L. N.; Tao, Y. T.; Ma, D. G.; Shuai, Z. G.; Qin, J. G. *Adv. Funct. Mater.* **2007**, *17*, 651.
4. Baldo, M. A.; Adachi, C.; Forrest, S. R. *Phys. Rev. B* **2000**, *62*, 10967.
5. Gong, X.; Ostrowski, J. C.; Bazan, G. C.; Moses, D.; Heeger, A. J.; Liu, M. S.; Jen, A. K.-Y. *Adv. Mater.* **2003**, *15*, 45.
6. Lee, C.-L.; Lee, K. B.; Kim, J.-J. *Appl. Phys. Lett.* **2000**, *77*, 2280.
7. Furuta, P. T.; Deng, L.; Garon, S.; Thompson, M. E.; Frechet, J.

M. J. *J. Am. Chem. Soc.* **2004**, *126*, 15388.
8. Park, M.-J.; Lee, J.; Kwak, J.; Jung, I. H.; Park, J.-H.; Kong, H.; Lee, C.; Hwang, D.-H.; Shim, H.-K. *Macromolecules* **2009**, *42*, 5551.
9. Xu, F.; Kim, H. U.; Mi, D.; Lim, J. M.; Hwang, J. H.; Cho, N. S.; Lee, J.-I.; Hwang, D.-H. *Bull. Korean Chem. Soc.* **2013**, *34*, 399.
10. Guan, R.; Xu, Y.; Ying, L.; Yang, W.; Wu, H.; Chen, Q.; Cao, Y. *J. Mater. Chem.* **2009**, *19*, 531.
11. Hertel, D.; Setayesh, S.; Nothofer, H.-G.; Scherf, U.; Müllen, K.; Bässler, H. *Adv. Mater.* **2001**, *13*, 65.
12. Evans, N. R.; Devi, L. S.; Mak, C. S. K.; Watkins, S. E.; Pascu, S. I.; Köhler, A.; Friend, R. H.; Williams, C. K.; Holmes, A. B. *J. Am. Chem. Soc.* **2006**, *128*, 6647.
13. Xu, F.; Lim, J. M.; Kim, H. U.; Mi. D.; Lee, J. Y.; Joo, C. W.; Cho, N. S.; Lee, J.-I.; Hwang, D.-H. *Synth. Met.* **2012**, *162*, 2414.
14. Chen, X.; Liao, J.-L.; Liang, Y.; Ahmed, M. O.; Tseng, H.-E.; Chen, S.-A. *J. Am. Chem. Soc.* **2003**, *125*, 636.
15. Nonoyama, M. *J. Organomet. Chem.* **1975**, *86*, 263.
16. Jiang, J.; Jiang, C.; Yang, W.; Zhen, H.; Huang, F.; Cao, Y. *Macromolecules* **2005**, *38*, 4072.
17. Chen, Y.-C.; Huang, G.-S.; Hsiao, C.-C.; Chen, S.-A. *J. Am. Chem. Soc.* **2006**, *128*, 8549.
18. Sun, Q. J.; Wang, H. Q.; Yang, C. H.; Li, Y. F. *J. Mater. Chem.* **2003**, *13*, 800.
19. Oh, H.-Y.; Lee, C.; Lee, S. *Org. Electron*. **2009**, *10*, 163.
20. Zhang, K.; Chen, Z.; Zou, Y.; Gong, S.; Yang, C.; Qin, J.; Cao, Y. *Chem. Mater.* **2009**, *21*, 3306.
21. Jiang, J.; Xu, Y.; Yang, W.; Guan, R.; Liu, Z.; Zhen, H.; Cao, Y. *Adv. Mater.* **2006**, *18*, 1769.